International Scientific Colloquium
**Modelling for Material Processing**
Riga, September 16-17, 2010

# A Physical Model for Electromagnetic Control of Local Temperature Gradients in a Czochralski System

## A. Cramer, M. Röder, J. Pal, G. Gerbeth

### Abstract

The shape of the solidification front and the related mono-crystalline growth in the Czochralski crystal growth process is thought of being strongly influenced by the ratio of the horizontal and the vertical temperature gradient $r^* = \Delta T_h / \Delta T_v$ at the triple point liquid-solid-atmosphere, which ratio desirably should be in the order of unity. A liquid metal model experiment was therefore built that allows studying $r^*$ under the influence of magnetic fields. The cylindrical liquid metal column was homogeneously heated from below, whereas on top the heat was extracted in a centre region covering only one third of the surface in order to simulate the growing crystal. Without flow control, $r^* \approx 3$ is far removed from unity. It was then possible to reach the target value $r^* = 1$ for any temperature difference between the bottom and the top at a moderate field strength while applying a rotating magnetic field.

### Introduction

Electromagnetic processing of materials provides the means to gain control of the flow in metallurgical and crystal growth tasks. Still to date, the strategy in quite a lot of work done on the field is to apply magnetic fields, observe their influence on the flow field, and to analyse the modification of the final product. A more promising approach goes the opposite direction: as flow control is merely a tool, the goal is to be expressed with objective functions. These targets are most reasonably formulated in terms of the relevant quantities, which are often distribution and transport of the scalars temperature and concentration. One example in Czochralski crystal growth, which was chosen as the subject of the present work, is the ratio $r^* = \Delta T_h / \Delta T_v$ of the horizontal and the vertical temperature gradient within the silicon melt at the perimeter of the growing crystal. Another instance of an objective function, to remain with crystal growth, may be derived also from the flow field: doubtlessly, the degree of turbulence in the vicinity of the crystal is important because a certain threshold exists, above which it is impossible to achieve mono-crystalline growth at all. However, the particular kind of a target is without loss of generality as it boils down to a question of measurability of the corresponding quantities, which is often accomplishable in the framework of physical modelling in the reduced temperature range.

Once an objective function is defined, the task formulation is to solve a multi-step inverse problem: A flow field that fulfils the target function is to be sought. Given this flow field, it has to be realised by means of applying magnetic fields, or, as is the case in crystal growth, the buoyant convection intrinsic to the process is to be accordingly controlled electromagnetically. Finally, a coil system producing the fields determined in the previous step has to be designed. Such an approach is desirably expressed analytically and/or numerically, which then might be even used to establish a transient control of the process. As

the problem is, however, extraordinarily difficult if ever solvable, known results from the corresponding forward strategies are to be adopted for each step.

Prior describing the apparatus employed to study the effect of the rotating magnetic field (RMF) used hitherto on the ratio $r^*$, the action of this field type on a cylindrical liquid metal volume is briefly recalled. An AC magnetic field of strength $\boldsymbol{B}_0$ applied to an electrical conductor induces an eddy current $\boldsymbol{j}$ within that medium. The interaction of $\boldsymbol{j}$ with the field that produced it results in a Lorentz force $\boldsymbol{F}_\mathrm{L} = \boldsymbol{j} \times \boldsymbol{B}_0$, which may drive a flow in the case that the electrical conductor is liquid. $\boldsymbol{F}_\mathrm{L}$ may be expressed as

$$\boldsymbol{F}_\mathrm{L} = \mathrm{Ta}\, r\, \varsigma(r,z)\boldsymbol{e}_\varphi, \quad \mathrm{Ta} = \frac{\sigma\omega B_0{}^2 \mathrm{R}^4}{2\rho\nu^2}, \tag{1}$$

where the Taylor number Ta is a measure for the relative strength of the driving force, $\sigma$, $\rho$, and $\nu$ are electrical conductivity, density and kinematical viscosity of the melt, r and R are the radial coordinate and the radius of the liquid metal column, and $\omega = 2\pi f$ is the frequency of the RMF [1]. The shape function $\varsigma$ vanishes at the top and the bottom walls while it depends only on R and the height of the liquid volume. Equation (1) is valid for the low-frequency and the low-induction approximations. Low frequency means $\mu\sigma\omega\mathrm{R}^2 < 1$ with $\mu$ being the magnetic permeability, whereas low-induction stands for the case that the characteristic angular velocity of the resulting flow is much smaller than the field frequency $\omega$. The flow developing under the influence of an RMF is a primary swirl following the mere azimuthal direction of $\boldsymbol{F}_\mathrm{L}$ in (1). Initiated by an imbalance between pressure and centrifugal force at non-vertical rigid walls, a meridional motion is superimposed. This secondary flow exhibits a toroidal structure with two vortices lying on top of each other, leading to a jet moving radially outward at mid-height of the liquid column [2].

## 1. Experimental Setup

The apparatus is a modified Rayleigh-Bénard configuration, in which the upper thermal boundary condition in a Czochralski system is accounted for by a partially cooled surface. This partial cooling covering approximately the same area as the growing crystal in an industrial facility is realised with a circular heat exchanger mounted concentrically within the upper lid. Some compromise had however to be made with respect to the entity of all boundary conditions. The surface between the crystal and the crucible is free, whereas it is covered by a PTFE lid in the model. This construction was motivated by the thermal boundary condition. In the reduced temperature range of the model, heat transport via radiation is negligible compared to the industrial case. As metallic melts at low temperatures are prone to oxidation, the surface would anyway not be sensitive to Marangoni convection. So it made sense to obey, at least, the thermal condition by allowing some heat flux from the melt into the lid simulating the radiation present in the industrial process. Both top heat exchanger and bottom heating plate are made from copper to approximate isothermal boundary conditions. This approach is further supported by a branched structure of flow channels machined into the copper parts. A precise control of temperatures is realised by supplying the heat exchanger and the bottom heater with coolant/heating fluid at high flow rate from thermostats having a large reservoir, the latter being regulated by a PID circuit. Differences

Fig. 1. Photo of the experimental setup

to the set-point and inhomogeneity were monitored by platinum resistance wires mounted within the heat exchanger and the bottom heater at various positions and found to be less than 0.05 K. Water may be used as a coolant, whereas the aim to reach high temperature gradients necessitates a heating fluid with a high boiling point. (silicone oil AK100, Wacker Chemitronic). It is noted that all copper parts in contact with the fluid are covered by a thin electrically insulating layer of aluminium oxide. Otherwise electric current may circulate between the fluid under investigation and those parts, which is likely to modify the distribution of the Lorentz force and in turn the flow structure.

The photo of the experimental cell in Fig. 1 shows that the side wall is transparent. A borosilicate glass pipe 90 mm in inner diameter and also 90 mm in height was chosen for the reasons of being electrically insulating, relatively poor heat conducting so as to approach adiabatic boundary condition, allowing transmission of ultrasound for flow measurements, and standing elevated temperatures. Sealing of the cell is realised by clamping the glass cylinder between the bottom heater and the PTFE top cover by means of thread rods screwed into the bottom plate. Different thermal expansion coefficients of the constructional materials are accounted for with springs inserted between the PTFE disc and the upper fastening nuts. The upper limit on temperature is imposed by the o-rings, which are located in the annular grooves machined into the PTFE disc (c.f. Fig. 3) and the bottom heater. These sealings are made from highly fluorinated synthetic elastomer and may be used at permanent load up to 280 °C. During the measurements, the whole apparatus was embedded in mineral wool serving the minimisation of lateral heat loss.

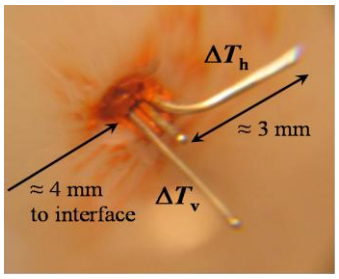


Fig. 2. (left): Equilateral-triangular arrangement of the three thermocouples comprising a measuring point

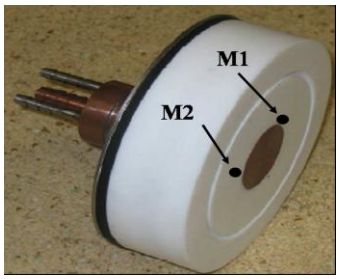


Fig. 3. (right): Oblique view from below of the PTFE top cover. M1 and M2 are the locations of the thermocouple-tripods close to the circumference of the heat exchanger

Temperatures in the melt are measured with mineral insulated type K thermocouples with protective tubes of 250 μm in total diameter. Three thermocouples in a triangular arrangement (c.f. Fig. 2) allow determination of both horizontal and vertical temperature gradients. Fig. 3 shows that two such tripods are mounted at the perimeter of the top heat exchanger. As we shall see next, the advantage thereof is not restricted to having solely a second measuring station. Because of the relatively small size of the thermocouples, transients of temperature may be recorded together with the mean values. Albeit flow measurement was not of primary importance, ultrasonic Doppler velocimetry in conjunction with the presence of two metering points for the temperature gradients proved a valuable tool in the detection and the characterisation of non-axisymmtric convective patterns. Acoustic properties of the borosilicate glass and the smooth surface of the pipe permit attaching a transducer to the outside of that wall to measure the radial velocity component along the entire ultrasonic beam. UDV has matured during the past years and is commercially available from a variety of manufacturers to date. Here, a DOP2000 (Model 2032, Signal-Processing, Lausanne, Switzerland) was used. The principle of operation of UDV is described in the pioneering work of Takeda [3], and a demonstration of the ability to work for liquid metals may be found in [4].

The rotating magnetic field was generated by the home-made MULTIpurpose MAGnetic field system, which is described in detail in [5]. Besides an RMF, MULTIMAG offers

also a travelling magnetic field, a single-phase alternating field, static fields in the variants of cusp-type and homogeneous field, and linear superpositions thereof. Such flexibility will certainly be the experimental basis for future work on the present topic of tailored flow control. The maximum value of the Taylor number in the present experimental setup is $\mathrm{Ta}^{\mathrm{max}} = 4 \cdot 10^9$.

## 2. Results and Discussion

The first series of measurements covered the flow without electromagnetic control. The only parameter subject to variation was the total temperature drop $\Delta T$ between the bottom heater and the top heat exchanger. Even though the surface was cooled only partially, the system may be described by the Grashof number

$$\mathrm{Gr} = \frac{\beta \mathrm{g} \Delta T \mathrm{H}^3}{\nu^2}, \tag{2}$$

where $\beta$, g, and H are volumetric expansion coefficient, acceleration of the free fall, and height. For Rayleigh-Bénard systems with homogeneous upper and lower temperature boundary conditions, a flow phenomenon often termed wind is known. Instead of an axi-symmetric convective pattern, fluid rising in a more or less kidney-shaped region at one side, moving along the surface to the opposing side, descending there, and closing the loop along the bottom is frequently observed. It was not expected to find such a wind in the system with partially cooled surface because of the primary strong horizontal temperature gradient at the perimeter of the heat exchanger directed radially everywhere, which gradient should lead to kind of a forced symmetrisation. Quite the contrary, the wind always showed up as the sole and stable flow pattern for all Gr albeit in statistical

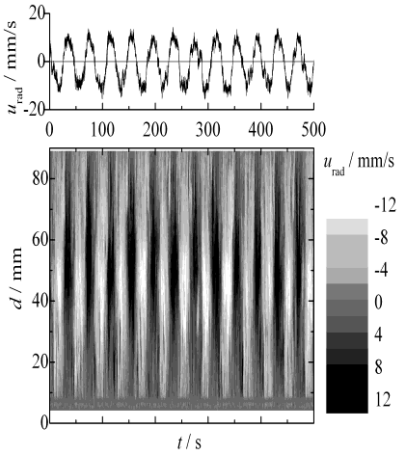


Fig. 4. Dependence of the radial velocity component on time at $\mathrm{Ta} = 5 \cdot 10^5$ in a contour plot along the ultrasonic beam (lower panel) and for a selected location (upper panel). While the RMF is weak the buoyant wind co-rotates with the magnetic field

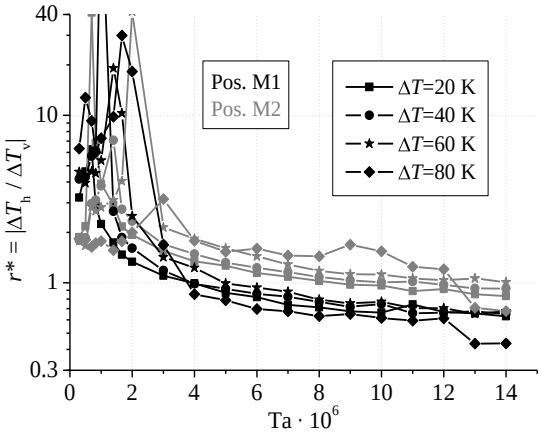


Fig. 5. Dependence of the objective function $r^*$ on the strength of the RMF

orientation. This mono-cellular pattern was first detected as an asymmetry in the temperature data recorded with both tripods, and later on confirmed by UDV measurements.

When the RMF is switched on, the wind starts to rotate. By analogue with the superposition of the primary and the secondary flow in an RMF, the swirl evoked by the RMF is also superimposed to the wind without any remarkable interaction. Not until the weaker secondary flow produced by the RMF becomes similar in vigour to the buoyant wind does the flow

structure in the modified Rayleigh-Bénard system change basically. The scenario for strengths of the RMF below this threshold is shown in Fig. 4 in the form of a spatio-temporal representation of velocity.

The objective function without applying the RMF is $r^* \approx 3$. It is reminded that it should not be expected to observe highly precise and reproducible values for that magnitude. $r^*$ is calculated from two differences out of three absolute measurements of temperature, each of the differences being quite small because of the short distance between the thermocouples. However, Fig. 5 evinces that $r^*$ deteriorates for weak magnetic fields up to the threshold described above in the previous paragraph. Although the representation of the ordinate is logarithmic, the plot is cropped at the upper end – $r^*$ reached values exceeding 100. Increasing the field strength leads to the secondary flow produced by the RMF dominating the wind; $r^*$ starts to decrease. As the mono-cellular buoyant flow structure vanishes completely above a certain value of Ta, Fig. 5 clearly shows that $r^* \approx 1$ is accomplishable whatever the vertically applied temperature difference. MULTIMAG would allow raising Ta for more than two orders of magnitude while the four $\Delta T$ contained in Fig. 5 are yet in the range of industrial interest ($Gr_{\Delta T=20K} = 1.7 \cdot 10^8$ … $Gr_{\Delta T=80K} = 1.1 \cdot 10^9$).

It is well known that an RMF may reduce the temperature fluctuations, which are inherent to turbulent natural convection. Hence, it was worthwhile to study also the transients of temperature. Fig. 6 shows the temperature signals recorded with one of the six thermocouples comprising the two tripods. The amplitude of the fluctuations decreases to 7 % when the field strength is increased about 50 times. Note that the higher value of $\boldsymbol{B}$ still is not what might be referred to as a strong field. A more detailed presentation of the results from temperature measurements covering four different values of the Grashof number are to be seen in Fig. 7. A common feature of the reduction of the temperature fluctuations for all Gr is that the absolute value of the normalised standard deviation $sd_T/\Delta T$ decreases to about 50 % and asymptotically approaches a value that is also common to any Gr.

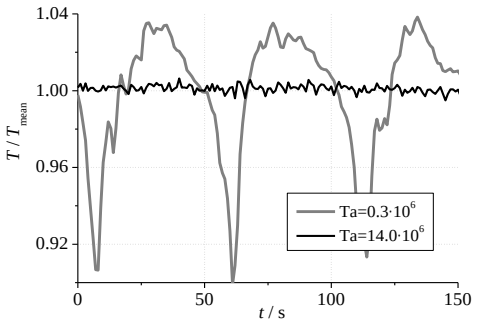


Fig. 6. Temperature signals recorded at two different strengths of the magnetic field

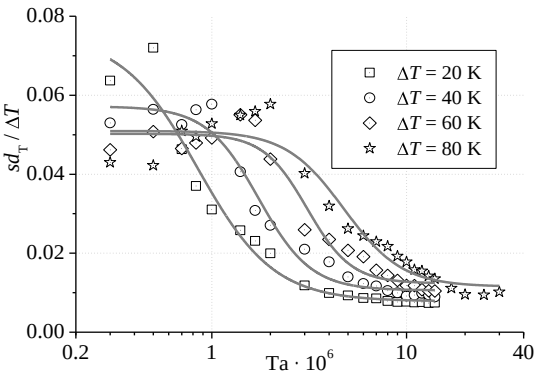


Fig. 7. Temperature fluctuation vs. magnetic forcing at different temperature gradients

**Summary and Perspectives**

Local temperature gradients and temperature fluctuations in the vicinity of the solid-liquid interface were studied at a physical model of the Czochralski crystal growth process. A comparable magnitude of the horizontal $\Delta T_h$ and the vertical temperature gradient $\Delta T_v$ at the triple point melt-crystal-atmosphere was chosen as the target function for an optimisation utilising electromagnetic flow control. It is shown that this task may be accomplished with a rotating magnetic field (RMF) alone: for any vigour of the intrinsic buoyant convection, it was always possible to adjust the RMF in such a way that $\Delta T_h \approx \Delta T_v$. The application of the RMF also reduced the temperature fluctuations.

Reaching a commensurate ratio of the temperature gradients with an RMF alone is, however, always at the expense of diminishing $\Delta T_h$. A smaller temperature gradient is, in general, likely to reduce the solidification rate. Therefore, investigations with other field types and combinations thereof aiming at an increase of $\Delta T_v$ are on the way.

A second generation experimental facility shown in Fig. 8 is close to completion, which will permit including the effects of crystal and/or crucible rotation. Thanks to a modular construction, it will allow to use various models of *crucibles* spanning from a generic Rayleigh-Bénard configuration to such ones being very similar to those used in the practice of industrial crystal growth (c.f. Fig. 9).

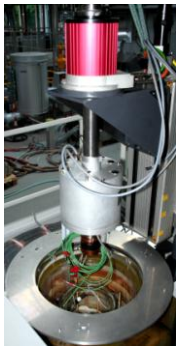

Fig. 8. General view at the second generation facility. The torque motor on top is responsible for the *crystal* rotation and the grey cylinder in the centre is a distributing jumper ring establishing electric contacts between rigid and movable parts incl. UDV signals in the MHz range

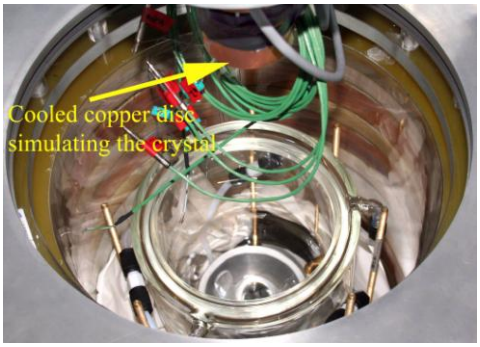


Fig. 9. Close-up of a *concept to reality* crucible mounted in MULTIMAG. The double-walled containment, which is thermostatically controlled with heated silicone oil, is independently rotatable by means of a rotary feedthrough installed below the magnet system

## References

[1] Gorbatchev, L. P., Nikitin, N. V., Ustinov, A. L.: *Magnetohydrodynamic rotation of an electrically conductive liquid in a cylindrical vessel of finite dimension*. Magnetohydrodynamics, Vol. 10, 1974, No. 3, pp. 406-414.

[2] Davidson, P. A., Hunt, J. C. R.: *Swirling, recirculating flow in a liquid metal column generated by a rotating magnetic field*. J. Fluid Mech., Vol. 185, 1987, pp. 67-106.

[3] Takeda, Y.: Development of an ultrasound velocity profile monitor. *Nucl. Eng. Des*., Vol. 126, 1991, pp. 277–284.

[4] Cramer, A., Zhang, C., Eckert, S.: *Local flow structures in liquid metals measured by ultrasonic Doppler velocimetry*. Flow Meas. Instrum., Vol. 15, 2004, pp. 145–153.

[5] Pal, J., Cramer, A., Gundrum, Th., Gerbeth, G.: *MULTIMAG - A MULTIpurpose MAGnetic system for physical modelling in magnetohydrodynamics*. Flow Meas. Instrum., Vol. 20, 2009, pp. 241-251.

## Authors

Dr. rer nat. Cramer, Andreas, Dipl.-Ing. Röder, Michael, Dr. rer nat. Pal, Josef, and Dr. rer nat. Gerbeth, Gunter
Department of Magnetohydrodynamics
Institute of Safety Research
Forschungszentrum Dresden-Rossendorf
P.O. Box 51 01 19
D-01314 Dresden, Germany
E-mail: a.cramer@fzd.de, m.roeder@fzd.de, j.pal@fzd.de, g.gerbeth@fzd.de